ChemPubSoc Europe

DOI: 10.1002/chem.201405340

CHEMISTRY A European Journal Full Paper

Isomerisation | *Hot Paper*

Dihydrogen Catalysis of the Reversible Formation and Cleavage of C–H and N–H Bonds of Aminopyridinate Ligands Bound to (η^5-C_5Me_5)Ir^{III}

Ana Zamorano, Nuria Rendón, Joaquín López-Serrano, José E. V. Valpuesta, Eleuterio Álvarez, and Ernesto Carmona*[a]

Abstract: This study focuses on a series of cationic complexes of iridium that contain aminopyridinate (Ap) ligands bound to an (η^5-C_5Me_5)Ir^{III} fragment. The new complexes have the chemical composition [Ir(Ap)(η^5-C_5Me_5)]$^+$, exist in the form of two isomers (**1**$^+$ and **2**$^+$) and were isolated as salts of the BAr_F^- anion (BAr_F = B[3,5-$(CF_3)_2C_6H_3]_4$). Four Ap ligands that differ in the nature of their bulky aryl substituents at the amido nitrogen atom and pyridinic ring were employed. In the presence of H_2, the electrophilicity of the Ir^{III} centre of these complexes allows for a reversible prototropic rearrangement that changes the nature and coordination mode of the aminopyridinate ligand between the well-known κ^2-*N*,*N*′-bidentate binding in **1**$^+$ and the unprecedented κ-*N*,η^3-pseudo-allyl-coordination mode in isomers **2**$^+$ through activation of a benzylic C–H bond and formal proton transfer to the amido nitrogen atom. Experimental and computational studies evidence that the overall rearrangement, which entails reversible formation and cleavage of H–H, C–H and N–H bonds, is catalysed by dihydrogen under homogeneous conditions.

Introduction

Half-sandwich rhodium and iridium complexes of the ancillary C_5Me_5 ligand are useful reagents for an ample variety of chemical transformations.[1] The steric protection that the permethylated cyclopentadienyl group provides and its excellent donor properties confer unique reactivity to complexes based on (η^5-C_5Me_5)M (M = metal) fragments and permit stabilisation of high-oxidation-state intermediates.[2,3a–d] Indeed, in recent decades compounds of this type have led to valuable discoveries in different areas of organometallic chemistry and catalysis. These comprise C–H bond-activation reactions,[4,5] cyclometallation reactions[1a,d] and a plethora of homogeneous catalytic reactions: water oxidation,[2,3] hydrogenation and hydrogen-transfer catalysis,[1b–e,6] hydrogen isotope exchanges[7,8] and other processes.[4e–f,9] Moreover, half-sandwich Rh and Ir derivatives, including [Ir(Cp′)(L^L′)X]$^{n+}$ complexes (Cp′ represents C_5Me_5 or C_5Me_4Ar (Ar = aryl or biaryl substituent), X is Cl^- or a related group and L^L′ is a bidentate C^N or N^N ligand) have been scrutinised with the aim of exploiting their esteemed properties as anti-cancer drugs and cell-imaging agents,[10a] and as hosts in molecular-recognition studies.[10b]

Recently, we have investigated the potential of (η^5-C_5Me_5)M^{III} complexes of Rh and Ir that contain cyclometallated phosphines as stoichiometric and catalytic reagents in C–H and H–H bond-activation reactions. We have also examined other relevant applications, such as catalytic hydrogen-isotope exchange, hydrosilylation of carbonyl groups and other unsaturated functionalities, as well as the formation of C–C bonds.[5d,8a–b,11,12] Related complexes that accommodate N^N or N^C mono-anionic ligands, rather than P^C ligands, also display rich and versatile chemistry.[1,2,6]

Accordingly, we commenced an investigation of the chemistry of complexes in which the (η^5-C_5Me_5)M^{III} core is stabilised by coordination to an aminopyridinate (Ap) ligand (Figure 1).[13,14] Besides finding great utility for stabilisation of complexes of electropositive metals (early-transition elements

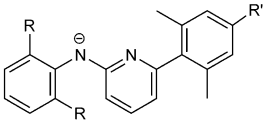

R	R′	
*i*Pr	H	**a**
Me	H	**b**
Me	NMe_2	**c**
Me	F	**d**

Figure 1. Aryl-substituted aminopyridinate ligands employed in this work.

[a] *Dr. A. Zamorano, Dr. N. Rendón, Dr. J. López-Serrano, Dr. J. E. V. Valpuesta, Dr. E. Álvarez, Prof. Dr. E. Carmona*
Instituto de Investigaciones Químicas (IIQ)
Departamento de Química Inorgánica and
Centro de Innovación en Química Avanzada (ORFEO-CINQA)
Consejo Superior de Investigaciones Científicas (CSIC)
and Universidad de Sevilla, Av. Américo Vespucio 49
Isla de la Cartuja, 41092 Sevilla (Spain)
Fax: (+34) 954460565
E-mail: guzman@us.es

Supporting information for this article is available on the WWW under http://dx.doi.org/10.1002/chem.201405340.

and some lanthanides),[14,15] latterly these ligands have been employed, mainly by Kempe and co-workers, to stabilise the quintuple Cr–Cr bond.[16] Similarly to other ligands of the amino-amide type, for instance $H_2NCH(Ph)CH(Ph)NTs^-$ (Ts = tosyl),[6] the amido terminus of aminopyridinates can function as a σ-donor and/or π-donor ligand depending upon the electronic requirements of the bound metal atom.[17] This electronic versatility facilitates some important transformations, such as the activation of H_2 and other small molecules, and explains the high efficiency of many group 8 and 9 metal complexes with amine-amido ligands as bifunctional molecular catalysts for hydrogen transfer and heterolytic hydrogenation reactions.[6,18,19]

In addition to compounds already cited, many Rh and Ir complexes of mono-anionic, chelating N^N ligands are known,[20] although information for M–Ap complexes is scarce.[21] Notwithstanding, preliminary work from our group[12] led to a cationic aminopyridinate complex $[Ir(Ap)(\eta^5\text{-}C_5Me_5)]^+$ (**1a**$^+$; Figure 1), which displays a five-coordinate structure but an eighteen-electron count thanks to the π-donor action of the aminopyridinate amido nitrogen atom.[12] Interestingly, besides irreversible reaction with H_2 to form the known binuclear compound[22] $[(\eta^5\text{-}C_5Me_5)Ir(\mu\text{-}H)_3Ir(\eta^5\text{-}C_5Me_5)]^+$ (isolated as the BAr_F^- salt; $BAr_F = B[3,5\text{-}(CF_3)_2C_6H_3]_4$), this complex undergoes spontaneous and reversible isomerisation of its aminopyridinate ligand from a classical κ^2-*N*,*N*′ coordination mode to an unprecedented κ-*N*,η^3-pseudo-allyl binding mode (Scheme 1) in a process efficiently catalysed by dihydrogen. Although coordination of H_2 to **1a**$^+$ and **2a**$^+$ was not observed, the corresponding carbonyl adducts **1a·CO**$^+$ and **2a·CO**$^+$ were isolated.[12]

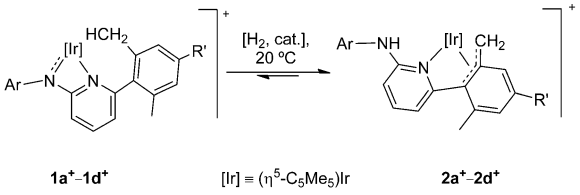

Scheme 1. The H_2-catalysed isomerisation of aminopyridinate ligands reported in this work. Ar is either 2,6-*i*Pr$_2$C$_6$H$_3$ or 2,6-Me$_2$C$_6$H$_3$.

Aside from playing a fundamental role in some biological processes,[23] the dihydrogen molecule is an indispensable reactant for homogeneous and heterogeneous catalytic processes of paramount importance.[24] Moreover, H_2 has become the ideal energy carrier.[25] Notwithstanding its significance, the catalytic action of H_2 is almost unknown.[12] We therefore decided to ascertain the generality of the H_2-catalysed rearrangement represented in Scheme 1. We have studied a series of $[Ir(Ap)(\eta^5\text{-}C_5Me_5)]^+$ complexes of substituted Ap ligands (Figure 1) and analysed their Lewis acid reactivity toward several Lewis bases. Most importantly, we have investigated their reactions with dihydrogen by experimental and computational methods. In this contribution we provide full details[12] of this work.

Results and Discussion

To broaden the utilisation of aminopyridinate ligands to the chemistry of late-transition metals, in particular to the coordination chemistry of the $(\eta^5\text{-}C_5Me_5)Ir^{III}$ fragment, and with the additional goal of ascertaining the generality of the H_2-catalysed isomerisation of aminopyridinate groups within an Ir–Ap linkage (Scheme 1), we studied iridium complexes of aminopyridinate ligands with diverse aryl substitution (Figure 1). The synthesis of ligand **a** was reported previously.[14] The remaining ligands **b**–**d** were obtained similarly, by a three-step procedure from the appropriate bromoaryl (Scheme 2 a) and aniline compounds (Scheme 2 c).

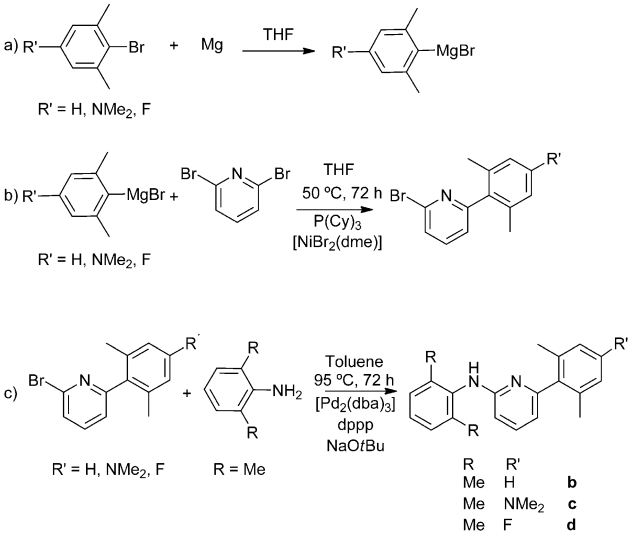

Scheme 2. Synthesis of the new aminopyridinate ligands employed in this work following the procedure reported in references [14a] and [14b]] for related ligands. $[Pd_2(dba)_3]$ = tris(dibenzylideneacetone)dipalladium(0), dppp = 1,3-bis(diphenylphosphanyl)propane.

Synthetic details are provided in the Supporting Information. The free amines, HAp, were isolated as white crystalline solids (the *p*-fluoro-substituted aminopyridine was characterised by X-ray crystallography; see Figure S1 in the Supporting Information) and generated in gram or multi-gram (5–10 g) quantities. The corresponding lithium amides, LiAp, were generated in situ prior to their use by the reported procedure.

Neutral and cationic $(C_5Me_5)Ir^{III}$–Ap compounds

The low-temperature (−50 °C) addition of a solution of LiAp in toluene to a suspension of the Ir^{III} dimer $[Ir(C_5Me_5)Cl_2]_2$ in the same solvent and subsequent stirring at room temperature for about 14 h permitted isolation of the yellow or orange crystalline complexes **1a·Cl**–**1d·Cl**, which exhibited the expected κ^2-*N*,*N*′ coordination of the aminopyridinate group (Scheme 3). In solution in CH_2Cl_2, these compounds readily underwent elimination of the chloride ligand by action of $NaBAr_F$ to form dark-grey, almost black, solutions of cations **1a**$^+$–**1d**$^+$, which were

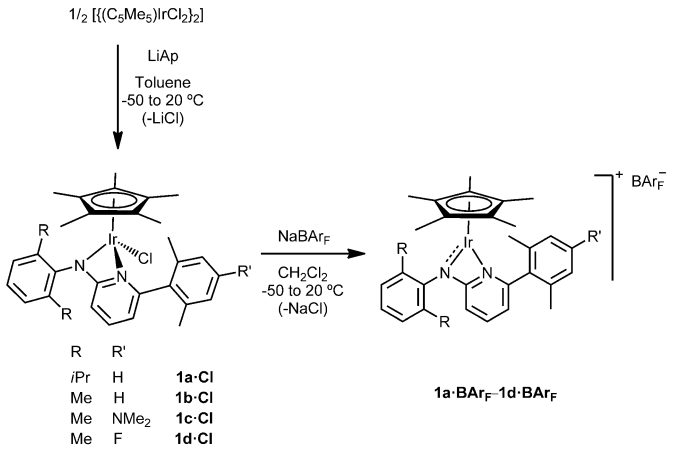

Scheme 3. Synthesis of neutral (**1 a·Cl**–**1 d·Cl**) and cationic (**1 a**$^+$–**1 d**$^+$) aminopyridinate complexes of the $(C_5Me_5)Ir^{III}$ fragment.

isolated as salts of the BAr_F^- anion. The base-free cations display five-coordinate structures but an electron count of eighteen on the assumption that the amido nitrogen atom behaves as a π-donor ligand toward the cationic Ir^{III} centre.[6,17] X-ray studies (see below) support this conjecture. Moreover, the very dark colour of these cations has been previously observed for complexes with M–N and M–O bonds stabilised by π donation and has been attributed to ligand-to-metal charge-transfer $\pi \rightarrow$d electronic transitions.[6a–e,17,26,27]

The neutral complexes **1 a·Cl**–**1 d·Cl** and their corresponding cationic derivatives **1 a**$^+$–**1 d**$^+$ were characterised by conventional structural techniques. ^{1}H and ^{13}C NMR spectroscopic studies (1D and 2D experiments) provide convincing evidence for the formulation proposed in Scheme 3. The chlorides **1 a·Cl**–**1 d·Cl** are chiral at iridium and the lack of symmetry becomes apparent in their ^{1}H and ^{13}C NMR spectra. For instance, for **1 a·Cl**, which contains 2,6-*i*Pr$_2$C$_6$H$_3$ and 2,6-Me$_2$C$_6$H$_3$ (Xyl) aryl substituents, two septets ($\delta = 3.39$ and 4.42 ppm) and four doublet resonances ($\delta = 1.21$, 1.32, 1.36 and 1.41 ppm) are recorded for the *i*Pr groups along with two singlets ($\delta = 2.10$ and 2.67 ppm) attributed to the methyl groups of the Xyl ring. In contrast, the C_s symmetry of the cationic molecules of **1 a**$^+$ is concluded from the observation of only one septet ($\delta =$ 3.61 ppm) and two doublets ($\delta = 1.15$ and 1.42 ppm) for the *i*Pr groups and one singlet ($\delta = 2.28$ ppm) for the Xyl methyl protons. Complete of NMR data for these complexes is provided in the Experimental Section.

The molecular structures of complexes **1 a·Cl**, **1 b·Cl**, **1 a**$^+$ and **1 d**$^+$ were determined by X-ray crystallography (Figure 2; Figures S3 and S5 in the Supporting Information). Besides the six-coordinate structures of the neutral chlorides compared with the less-common five-coordinate geometries of the cationic species, there are other significant structural differences that mainly concern the binding of the Ap ligand in the two types of compound. Thus, in the neutral derivatives, the Ir–N bond lengths for the pyridinic (N_{py}; N1 in Figure 2) and amido (N_{amido}; N2 in Figure 2) nitrogen atoms are quite similar, with the former ($\approx$2.15 Å) somewhat longer than the latter

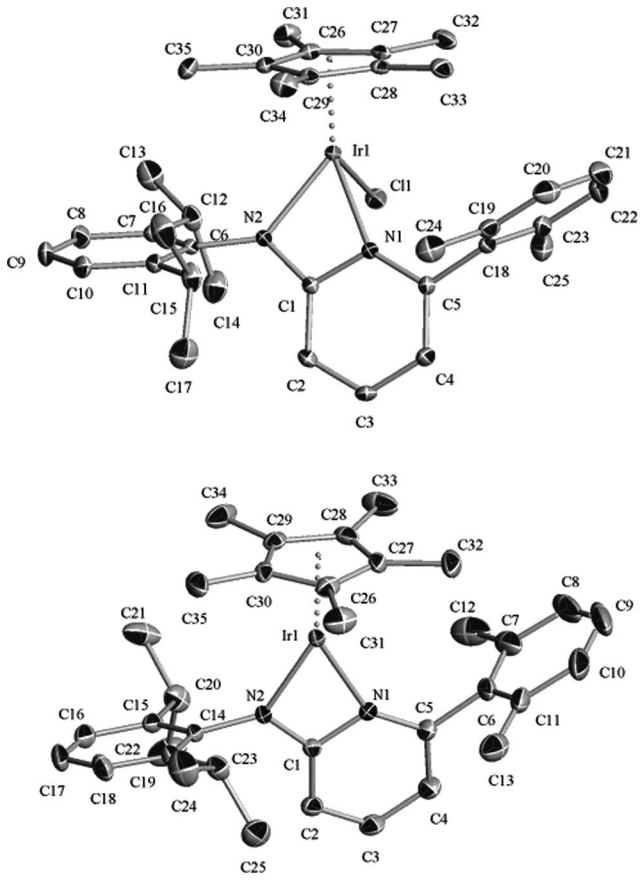

Figure 2. X-ray structures of complexes **1 a·Cl** (top) and **1 a**$^+$ (bottom). Anion BAr_F^- is omitted for clarity.

($\approx$2.11 Å), as expected. For the two cations **1 a**$^+$ and **1 d**$^+$ both the Ir–N_{py} and the Ir–N_{amido} bond lengths are shorter than in the neutral chlorides, most probably a consequence of the lower coordination number. Importantly, whereas the decrease in the Ir–N_{py} bond length is small (roughly 0.03 Å), that of the Ir–N_{amido} bond is much larger at 0.15 Å (for instance, 2.1085(17) Å in **1 a·Cl** and 1.965(2) Å in **1 a**$^+$). These data hint at significant Ir–N_{amido} π bonding in **1 a**$^+$ but less, or none, in **1 a·Cl**, a hypothesis that can be extended to the rest of the complexes in Scheme 3. The reactivity of the cationic complexes **1**$^+$ towards Lewis bases and natural bond order (NBO) analyses on model compounds (see below) furnish additional support for this proposal. These data compare well with those reported in the literature for somewhat related compounds.[6,28]

Lewis base adducts of cations $[Ir(Ap)(\eta^5\text{-}C_5Me_5)]^+$

As represented in Scheme 4 for **1 a**$^+$, addition of the N- and C-donors NH_3, 4-dimethylaminopyridine (DMAP), CO and CNXyl, led to an immediate and abrupt colour change from the very dark, nearly black colouration of **1 a**$^+$ to the yellow-orange characteristic colour of the six-coordinate adducts **1 a·L**$^+$. In addition to **1 a·CO**$^+$, the remaining carbonyl species **1 b·CO**$^+$ –**1 d·CO**$^+$ were also isolated.

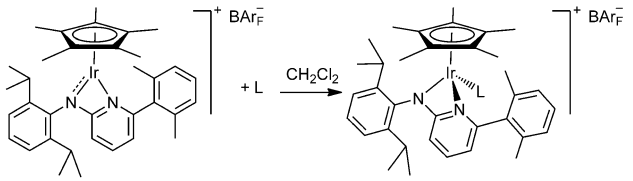

Scheme 4. Reactions of complex **1a**$^+$ with different Lewis bases.

The ammonia and DMAP derivatives, **1a·NH$_3$**$^+$ and **1a·DMAP**$^+$ exhibited dynamic behaviour at room temperature that was not investigated. The ^{1}H NMR spectrum of **1a·NH$_3$**$^+$ recorded at 0 °C (CD_2Cl_2, 500 MHz) features, in addition to signals due to the C_5Me_5 and Ap ligands (see the Experimental Section), a resonance at $\delta = 2.16$ ppm with a relative intensity that corresponded to three hydrogen atoms, which was assigned to the coordinated NH_3 molecule. Crystallographic analysis of the BAr_F salts of these cations (Figure 3) revealed unexceptional structural features. For example, the Ir–NH_3 bond of **1a·NH$_3$**$^+$ has a length of 2.164(5) Å, which is comparable to that found in other $(C_5Me_5)Ir^{III}$–NH_3 complexes.[6d,28d,29]

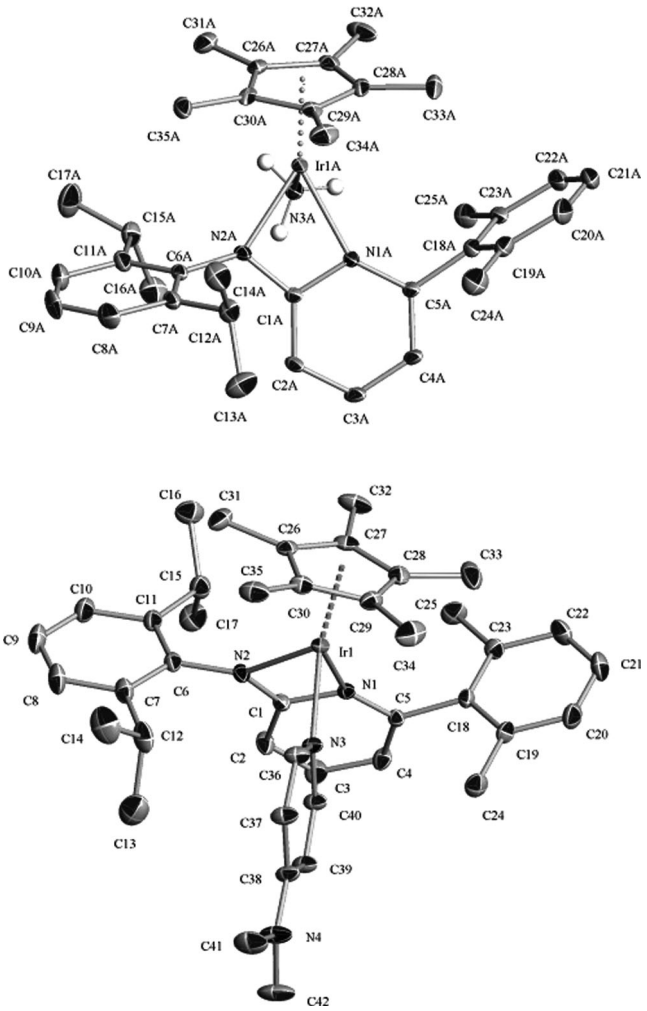

Figure 3. X-ray structures of complexes **1a·NH$_3$**$^+$ (top) and **1a·DMAP**$^+$ (bottom). Anion BAr_F^- is omitted for clarity.

The IR spectra of the carbonyl adducts **1a·CO**$^+$–**1d·CO**$^+$ exhibit the expected carbonyl stretching frequency that appears in the narrow interval $\tilde{\nu} = 2060$–2050 cm^{-1} (see Table S1 in the Supporting Information). In all likelihood, the high $\tilde{\nu}$(CO) values are a reflection of low back-donation from the cationic Ir^{III} centre to the π^* antibonding orbitals of the CO ligand. This is a common observation for many cationic Ir^{III}–CO complexes[6d,30] and, more generally, for cationic carbonyl complexes of the transition metals,[31] including other late-transition metals.[32] The subtle differences recorded for this series of complexes ($\Delta\tilde{\nu}$(CO) ≈ 10 cm^{-1}) are striking and do not appear to correlate with the electron-donor properties of the aminopyridinate aryl substituents. In particular, $\Delta\tilde{\nu}$(CO) between the *para*-NMe_2-substituted complex **1c·CO**$^+$ and the *para*-F-substituted analogue **1d·CO**$^+$ is only 3 cm^{-1}. This observation suggests that the pyridyl aryl substituents have little, or no, influence on the electron-donating properties of the aminopyridinate ligands. In fact, it is possible that the small changes measured for $\tilde{\nu}$(CO) in our complexes are meaningless in terms of M–CO electronic interaction and may be due to polarisation of the carbon–oxygen sigma bond of the coordinated molecule of CO by the positively charged Ir^{III} centre.[31] Crystallographic studies performed with the BAr_F^- salts of **1a·CO**$^+$ and **1b·CO**$^+$ (Figure 4) furnished Ir–CO distances of about 1.89 Å and C–O bond lengths of about 1.11 Å, which are consistent with the high $\tilde{\nu}$(CO) values observed and reinforce the notion of very low π basicity of the iridium centre in these complexes.[6d,30]

Solutions of **1a**$^+$ in dichloromethane were also reacted with stoichiometric amounts of the aryl isocyanide CNXyl. An instant reaction took place marked, once again by a noticeable colour change from black to yellow-orange, and provided the desired compound **[1a·CNXyl]BAr$_F$** in essentially quantitative yield. Aryl isocyanides are efficient π-acid ligands,[33] which act mostly, or exclusively, as σ donors when confronted with metal fragments of scarce π-donor capacity.[34] Similarly to CO, isocyanides bind to metal centres with donation of electron density from a molecular orbital polarised at the isocyanide carbon atom, which possesses some antibonding character. Accordingly, M←C≡NAr σ donation reinforces the C≡N bond and results in an increase of $\tilde{\nu}$(C≡N).[33,34] In the IR spectrum of **1a·CNXyl**$^+$, the target $\tilde{\nu}$(C≡N) band appears with a high wavenumber of 2155 cm^{-1}, which is roughly 40 cm^{-1} shifted toward higher energy relative to free CNXyl. Thus, the positive shift strengthens the perception of the very weak capability of a cationic $[Ir^{III}(Ap)(C_5Me_5)]^+$ core to act as a π donor toward efficient π-acid ligands like CO and aryl isocyanides. Figure 5 illustrates the molecular structure of **1a·CNXyl**$^+$, which exhibits Ir–N_{py} and Ir–N_{amido} bond lengths that match those determined for other **1a·L**$^+$ adducts and an Ir–CNXyl bond length of 1.961(2) Å, which is somewhat longer than the Ir–CO bond length in **1a·CO**$^+$ (1.884(7) Å).

Reactions of cationic complexes $[Ir(Ap)(\eta^5\text{-}C_5Me_5)]^+$ with H_2

The study of the reactivity of transition-metal complexes with the dihydrogen molecule is an essential part of organometallic chemistry because the resulting hydride or dihydrogen com-

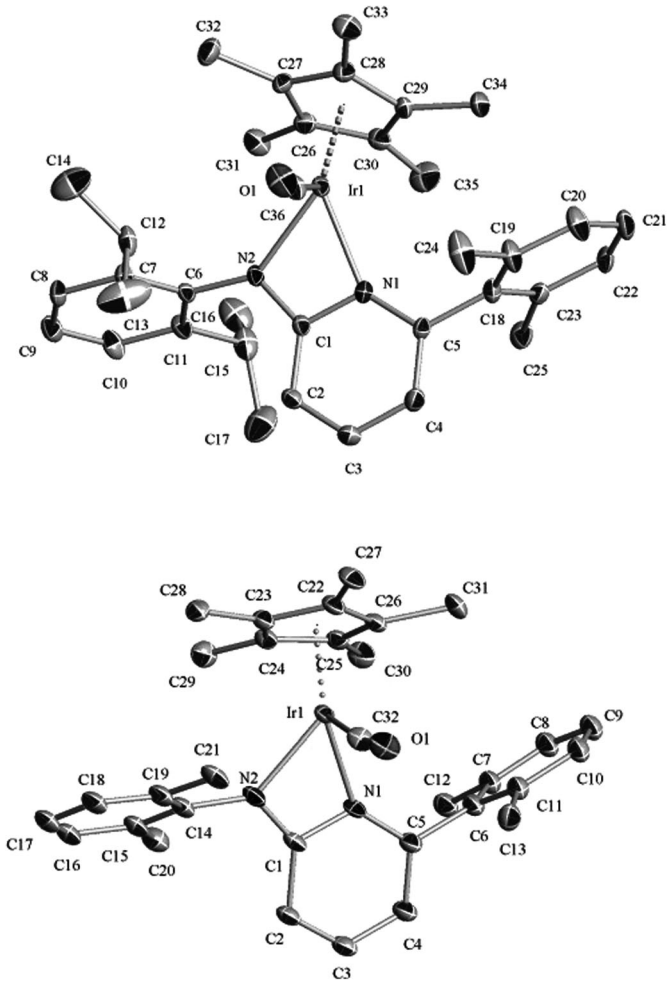

Figure 4. X-ray structures of complexes **1a·CO**$^+$ (top) and **1b·CO**$^+$ (bottom). Anion BAr_F^- is omitted for clarity.

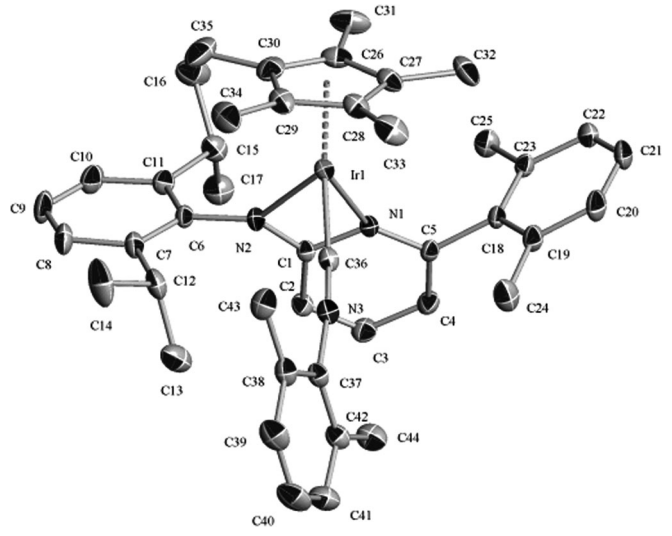

Figure 5. X-ray structure of complex **1a·CNXyl**$^+$; anion BAr_F^- is omitted for clarity.

plexes are often active participants in homogeneous catalytic reactions.[18a,23b,24b,35–38] The electrophilicity of the five-coordinate complexes **1a**$^+$–**1d**$^+$, evidenced in the reactivity studies already discussed, prompted us to investigate their interaction with H_2. As depicted in Scheme 5, all complexes reacted irreversibly at room temperature with an excess of H_2 to produce the known[22] binuclear hydride complex $[\{(\eta^5\text{-}C_5Me_5)Ir\}_2(\mu\text{-}H)_3]BAr_F$, together with the corresponding free- and protonated-aminopyridine, HAp and $[H_2Ap]BAr_F$, respectively. For identification purposes, the formation of the latter species was monitored by ^{1}H NMR spectroscopy and its identity was confirmed by protonation of HAp with $HBAr_F$. Interestingly, since the early description of the above binuclear complex by Maitlis et al.[22] it has been identified as the product of hydrogenation of different cationic complexes of the $(\eta^5\text{-}C_5Me_5)Ir^{III}$ fragment.[3b,22b,39]

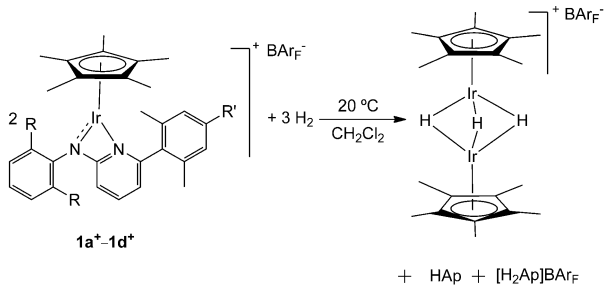

Scheme 5. Reaction of aminopyridinate complexes **1a**$^+$–**1d**$^+$ with an excess of dihydrogen.

The reactions of complexes **1**$^+$ with stoichiometric or substoichiometric concentrations of H_2 (Scheme 5) are fast once they start but feature ill-defined kinetics and may be avoided, particularly if low relative concentrations of H_2 (less than 40 mol%) are employed at room temperature or below. Under these conditions, an interesting and unprecedented reversible isomerisation of the Ir–Ap linkage of cations **1**$^+$ was observed (Scheme 1), which allowed for the isolation of complexes **[2a]BAr$_F$**–**[2d]BAr$_F$**. As can be seen, isomerisation of complexes **1**$^+$ necessitates benzylic C–H bond activation with formal proton transfer to the amido nitrogen atom, which becomes uncoordinated. Thus, the most characteristic details of the NMR spectra of the new complexes are those pertinent to these functionalities. For example, with reference to the equilibrium **1a**$^+$⇌**2a**$^+$ (Scheme 6) the singlet at $\delta = 2.28$ ppm due to the Xyl methyl protons of **1a**$^+$ (relative intensity = 6H) converts into a singlet ($\delta = 2.48$ ppm; 3H), two doublets ($\delta = 3.68$ and 2.07 ppm; 1H each; $^2J(H,H) = 4.5$ Hz) and one slightly broad resonance attributed to the amine proton of **2a**$^+$ ($\delta =$ 5.94 ppm; 1H). In the ^{13}C NMR spectrum of **2a**$^+$ the η^3-benzylic terminus is responsible for signals at $\delta = 100.4$ (Ir–CH_2C_q), 94.1 (Ir–C_q) and 34.9 ppm (Ir–CH_2; $^1J(C,H)_{average} = 155$ Hz).

The described rearrangement of the Ap ligand was structurally authenticated by X-ray studies of complexes **2a**$^+$–**2c**$^+$ (Figure 6; Figure S12 in the Supporting Information). In the three complexes, the Ir–N_{py} bonds have similar lengths (**2a**$^+$: 2.073(6) Å; **2b**$^+$: 2.098(4) Å; **2c**$^+$: 2.083(5) Å) and the Ir-(η^3-benzylic) moieties possess one relatively short Ir–CH_2 bond ($\approx$2.12 Å), an intermediate Ir–CH_2C_q distance of about 2.25–2.30 Å and a longer Ir···C_q contact of about 2.40 Å.

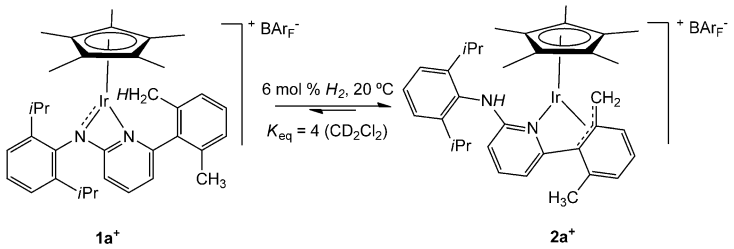

Scheme 6. Reversible isomerisation of complexes $\mathbf{1a}^+$ and $\mathbf{2a}^+$ catalysed by H_2.

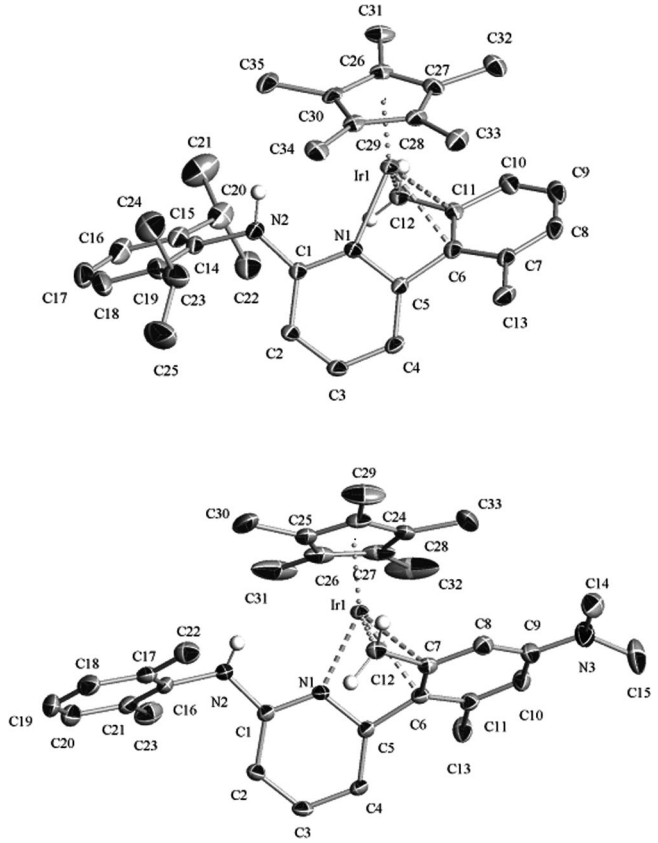

Figure 6. X-ray structures of complexes $\mathbf{2a}^+$ (top) and $\mathbf{2c}^+$ (bottom). Anion BAr_F^- is omitted for clarity.

Complexes $\mathbf{1}^+$ did not undergo any observable change upon prolonged stirring either at room temperature or 50–60 °C in the absence of H_2. Furthermore catalytic concentrations of H_2 as low as 2–5 mol% (measured by ^{1}H NMR spectroscopy in solution in CD_2Cl_2) efficiently promoted the $\mathbf{1}^+ \rightleftharpoons \mathbf{2}^+$ rearrangement, although longer reaction periods were needed. For instance, a H_2 load of about 1.6 mol% induced the $\mathbf{1a}^+ \rightleftharpoons \mathbf{2a}^+$ interconversion at 20 °C with a half-life ($t_{1/2}$) of about 9.1 h. Thus, the isomerisation of the aminopyridinate ligand of these complexes was catalysed by dihydrogen. Extensive preparative and NMR spectroscopic studies of this reaction system demonstrated that complexes $\mathbf{1a}^+$–$\mathbf{1d}^+$ exist in solution in dynamic equilibrium with their $\mathbf{2a}^+$–$\mathbf{2d}^+$ counterparts.

With the exception of the 4-dimethylamino-substituted complex $\mathbf{1c}^+$, which converts almost quantitatively (≥95% by ^{1}H NMR spectroscopy) into its $\mathbf{2c}^+$ isomer, the equilibria display little sensitivity to changes in the aminopyridinate aryl substituents, with values of $K_{eq} = 4 \pm 0.5$ for the $\mathbf{1a}^+/\mathbf{2a}^+$ and $\mathbf{1b}^+/\mathbf{2b}^+$ couples and of $K_{eq} = 2 \pm 0.5$ for the $\mathbf{1d}^+/\mathbf{2d}^+$ couple. The same equilibrium mixtures were reached starting from the pure η^3-benzylic complexes $\mathbf{2a}^+$, $\mathbf{2b}^+$ and $\mathbf{2d}^+$, although longer reaction times were needed. These K_{eq} values reveal that the two isomeric structures have similar thermodynamic stability, although in comparative terms the κ-*N*,η^3-pseudo-allyl Ap coordination mode in $\mathbf{2c}^+$ leads to enhanced stability, most likely due to the electron-donating properties of the *para*-NMe_2 substituent.

The rate of the $\mathbf{1}^+ \rightarrow \mathbf{2}^+$ redistribution reaction is dependent upon the H_2 concentration. Thus, $t_{1/2}$ values of about 2.5 h and 30 min were measured for the conversion of $\mathbf{1a}^+$ into $\mathbf{2a}^+$ at 20 °C in CD_2Cl_2 for concentrations of H_2 in solution of 6 and 32 mol%, respectively (see above for additional data). Although isomerisation rates were of comparable magnitude for all the compounds investigated, the $\mathbf{1a}^+ \rightleftharpoons \mathbf{2a}^+$ reorganisation was comparatively slower, perhaps due to steric hindrance exerted by the 2,6-$iPr_2C_6H_3$ aryl substituent. A sufficiently detailed kinetic study of the $\mathbf{1}^+ \rightleftharpoons \mathbf{2}^+$ interconversions was unfortunately unattainable. This was due to the somewhat erratic and unpredictable tendency of complexes $\mathbf{1}^+$ to react irreversibly with H_2 (discussed above) in the manner shown in Scheme 5.

Countless hydrogenation reactions both stoichiometric and catalytic are known. Even if it would not be surprising that a molecule of H_2 functions not only as a reagent but also as a catalyst, literature precedent for H_2-catalysed reactions is very limited.[12,40] In the system under scrutiny, H_2 behaves as an efficient homogeneous catalyst and promotes the formation and cleavage of C–H and N–H bonds of Ap ligands bound to the (η^5-C_5Me_5)Ir^{III} fragment. Sola and co-workers demonstrated a fast catalysis by H_2 of the *syn–anti* isomerisation of five-coordinate iridium mono-hydride complexes stabilised by κ^3-*P*,*P*′,Si-binding of the PSiP pincer ligand –Si(Me){$(CH_2)_3PPh_2$}$_2$.[41] In accordance with NMR spectroscopic and computational studies, no exchange between Ir–H and H_2 took place during the *syn–anti* isomerisation, although such an exchange could be possible in a low-energy tri-hydride intermediate.[41]

A series of experiments were developed to demonstrate beyond any doubt the proposed homogeneous and catalytic nature of the isomerisation depicted in Scheme 6.[42] The experiments included discarding a heterogeneous process[43] promoted by iridium colloidal particles, as well as unnoticed catalysis by water or other Brønsted–Lowry acids or bases.[6d,44] In addition, besides commercially available H_2 (and D_2, see below), dihydrogen was chemically generated by well-established procedures.[42] In the course of these experiments it was found that $\mathbf{1a}^+$ underwent no observable change when treated with H_2 in the presence of the weakly coordinating base TMPP (2,2,6,6-tetramethylpiperidine), whereas its pseudo-allylic isomer $\mathbf{2a}^+$ reacted to yield the neutral hydride **1a·H** (Scheme 7), which was alternatively generated by the action of $NaBH_4$ on the parent chloride **1a·Cl**. The analogous hydride **1b·H** was also obtained (see the Experimental Section).

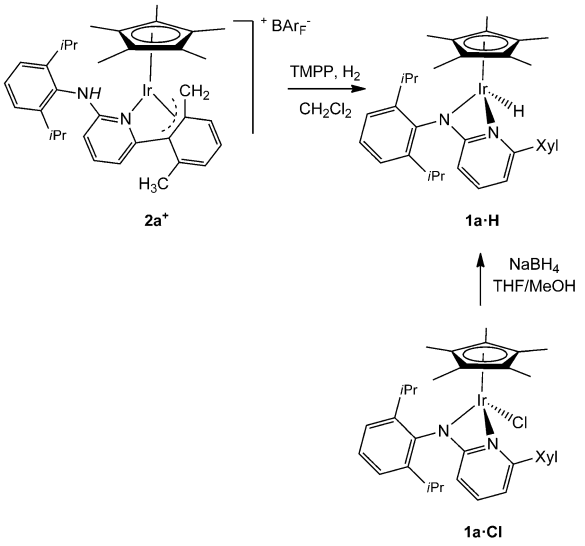

Scheme 7. Two different syntheses of the hydride complex **1a·H**.

Further experimental work was accomplished. Use of D_2 provided a kinetic isotopic effect (KIE) with $k_H/k_D = 1.3$, which suggested that H–H bond cleavage had no important contribution to the rate-determining step. KIE values close to 1 are commonly found for reactions of H_2 with unsaturated complexes.[34,45] When D_2 was utilised as the catalyst, selective deuterium incorporation was realised, firstly in complex **2a**$^+$ at the amido nitrogen atom (which converts into an amine, >NH or >ND) and the CH_2 and CH_3 sites of the metallated Xyl group, and secondly, if sufficient time was allowed, at the Xyl methyl positions of isomer **1a**$^+$.

The facile, H_2-promoted reversible rearrangement, **1**$^+$⇌**2**$^+$, suggested that similar to complexes **1**$^+$, the pseudo-allylic derivatives **2**$^+$ should also exhibit electrophilic character and react readily with Lewis bases with a concomitant benzylic coordination change from η^3 to κ-C. Bubbling CO through solutions of the two complexes chosen for this study, **2a**$^+$ and **2c**$^+$, in CH_2Cl_2 confirmed this prediction and led to quantitative formation of the carbonyl adducts **2a·CO**$^+$ and **2c·CO**$^+$ (Scheme 8). The two compounds display a strong IR absorption with nearly the same wavenumber ($\tilde{\nu}$(CO) = 2030 cm^{-1}; see Table S1 in the Supporting Information), which is somewhat shifted to lower energy relative to the corresponding band for isomers **1a·CO**$^+$ and **1c·CO**$^+$. The shift, albeit modest (20 cm^{-1} for the **1a·CO**$^+$/**2a·CO**$^+$ couple and 28 cm^{-1} for **1c·CO**$^+$/**2c·CO**$^+$), may be taken as suggestive of the moderately better electron-donating properties of the η^1-benzylic ligand in complexes **2·CO**$^+$ than for the N_{amido} functionality present in complexes **1·CO**$^+$.

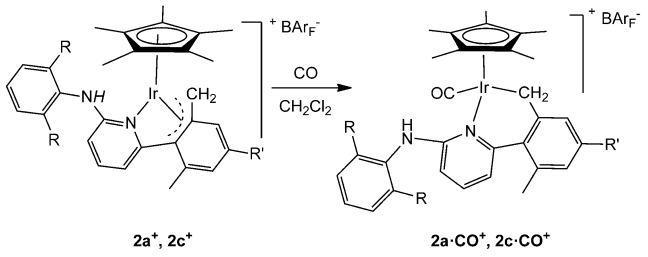

Scheme 8. Formation of carbonyl complexes **2a·CO**$^+$ and **2c·CO**$^+$.

In summary, some relevant characteristics of this unusual reaction system are:

1) The isomeric complexes **1**$^+$ and **2**$^+$ have similar thermodynamic stabilities.
2) In solution they exist in a dynamic equilibrium that can be reached starting from either side.
3) Isomer equilibration requires the formation and rupture of C–H and N–H bonds and occurs at room temperature or below under homogeneous dihydrogen catalysis.
4) Dihydrogen activation, that is H–H bond cleavage, is not rate limiting.

Computational studies and mechanistic proposal

With reference to complexes **1a**$^+$ and **2a**$^+$, chosen as models for this theoretical analysis, the experimental efforts to elucidate a mechanism for their isomerisation were completed with DFT (B3LYP) calculations. Initial explorations, previously communicated,[12] used a model system with a cyclopentadienyl (C_5H_5) instead of a C_5Me_5 ligand and two Xyl fragments on the aminopyridinate ligand (**Cp·1b**$^+$), but the results discussed herein correspond to calculations based on the cation complexes of the real species **1a**$^+$ and **2a**$^+$, unless stated otherwise. Thermodynamic data are relative free energies in the gas phase and energy barriers correspond to relative electronic energies in the gas phase.

The calculations at this level indicate that the energies of the two isomers are comparable, consistent with the two compounds existing in equilibrium; **1a**$^+$ is favoured over **2a**$^+$ by 3.1 kcal mol^{-1}. However this may be an effect of the functional. Use of M06, which has been claimed to give a better account of dispersive forces in large molecules[46] (see the Supporting Information), leads to a greater stability of **2a**$^+$ by 0.5 kcal mol^{-1}, and equates to an equilibrium constant of 2.3.

Despite experimental evidence that establishes a role for dihydrogen in the isomerisation, a mechanism was explored without H_2 participation and was discarded. Oxidative addition of one benzylic C–H bond of **1a**$^+$ has an energy barrier ($\Delta E^{\neq}$) of 38.1 kcal mol^{-1}, too high for a room temperature process. Furthermore, migration of the resulting iridium hydride to the amido nitrogen atom yields an even higher overall barrier from **1a**$^+$ of 45.1 kcal mol^{-1} (see Figure S15 in the Supporting Information).

The calculations indicate that H_2 coordination to **1a**$^+$ is endergonic ($\Delta G = 20.4$ kcal mol^{-1}) and the resulting dihydrogen complex (**A**) undergoes a reduction in the molecular symmetry (from C_s in **1a**$^+$ to C_1, see Figure 7) and an elongation of the Ir–N_{amido} bond from 1.98 to 2.15 Å. NBO analysis of the simplified model **Cp·1b**$^+$ showed that the natural localised molecular orbital (NLMO) derived from the lone pair on the amido nitrogen atom has a 10.2% contribution from Ir and 73.9% from

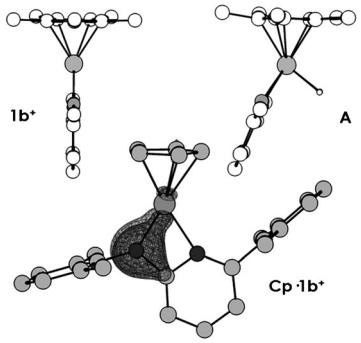

Figure 7. Views of the DFT-optimised structures of cations **1b**$^+$ (top left) and **A** (top right). The bottom structure shows the π (Namido-Ir) natural localised molecular orbital (NLMO) of **Cp·1b**$^+$ with a significant contribution from Ir.

its parent NBO. Upon H_2 coordination the contribution from Ir to the corresponding NLMO becomes less than 1%, which is consistent with a decrease in the double-bond character of the Ir–N_{amido} interaction in intermediate **A** and other adducts **1a·L**$^+$.

The dihydrogen intermediate **A** is in fast equilibrium with the corresponding Ir^V dihydride, **A**-(**H**)$_2$ according to the calculations, which predict that the dihydride complex is more stable ($\Delta G \approx 2$ kcal mol^{-1}). The activation of H_2 from **A** is almost barrier-less, however the overall barrier from **1a**$^+$ amounts to 20 kcal mol^{-1} (see Figure 8). Protonation of the N_{amido} atom takes place from the dihydride complex (see Figure 9; no transition state was located for the corresponding elemental step from the dihydrogen intermediate **A** at this level of theory) with a barrier of $\Delta E^{\neq} = 12.2$ kcal mol^{-1} (Figure 8). The resulting Ir^{III} monohydride (**B**) lies above **1a**$^+$ + H_2 ($\Delta G = 8.3$ kcal mol^{-1}) and features an interaction between the Ir atom and NH moiety (2.33 Å). The next step requires activation of one benzylic C–H bond (see Figure 9 for transition-state geometry) but needs a conformational change to replace the Ir–NH interaction with an η^2 interaction with the Xyl substituent of the pyridine moiety.[47] Calculations at various levels of theory and with different models suggest that the extent of

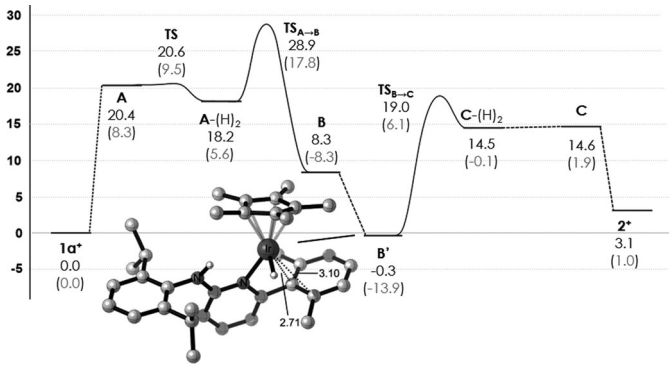

Figure 8. Calculated free energy profile (kcal mol^{-1}; data in parentheses correspond to electronic energies) of the dihydrogen-assisted isomerisation **1a**$^+$⇌**2a**$^+$. The inset represents the optimised geometries of the intermediate **B**′ (most hydrogen atoms are omitted). Calculated distances are in Å.

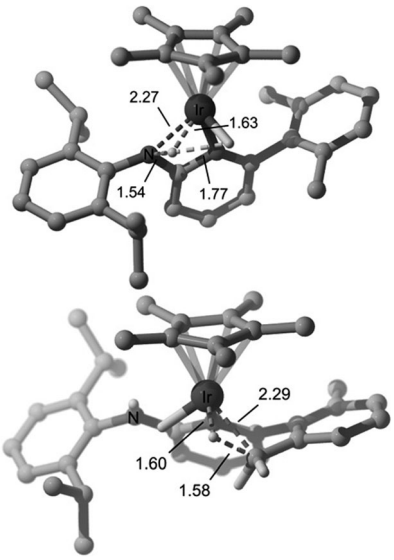

Figure 9. DFT-optimised geometries of the transition states for the protonation of the N_{amido} (**TS**$_{A\rightarrow B}$) and the activation of one benzylic C–H of **B**′ (**TS**$_{B\rightarrow C}$). Calculated distances are in Å.

this bond is dependent on the steric interaction between the C_5Me_5 and the Ap ligands (see the Supporting Information for details), whereas all calculations predict that species **B**′ has a relative energy comparable to (or lower than) that of **1a**$^+$ + H_2 (−0.3 kcal mol^{-1}).

Activation of one benzylic C–H unit of **B**′ yields a new Ir^V dihydride **C-(H)$_2$**, with a relative energy of 14.5 kcal mol^{-1}. This dihydride is in rapid equilibrium with the corresponding dihydrogen complex **C** (as in the case of **A** and **A-(H)$_2$**, the dihydride and the dihydrogen species have similar energies). Finally, the latter can eliminate H_2 to yield **2a**$^+$.

On the basis of the experimental and theoretical data presented thus far, the equilibrium between the isomeric species **1a**$^+$⇄**2a**$^+$ may occur as represented in Scheme 9. It seems likely that reactive, undetected iridium σ-dihydrogen complexes could be generated by coordination of dihydrogen to the electrophilic iridium centres of **1a**$^+$ and **2a**$^+$.[23b,35–37] Dihydrogen intermediates **A** and **C** would be structurally analogous to the adducts **1a·CO**$^+$ and **2a·CO**$^+$ discussed already. Protonation of the Ir–N_{amido} bond may occur by heterolytic rupture of the H–H bond to give H^-, which links to the metal with formation of the hydride ligand, and H^+, which migrates intramolecularly to protonate the amide group (intermediate **B**). Alternatively, homolytic rupture could occur to form a cationic bis-hydride complex of Ir(V). From **B**, activation of a C–H bond from a methyl group of the Xyl substituent followed by elimination of H_2 would lead to the η^3-benzylic isomer **2a**$^+$.

Conclusion

The experimental and computational studies described in this paper demonstrate that aminopyridinate ligands with a 2,6-dimethyl-substituted aryl group at the 6-position of the pyridinic terminus can bind to the (η^5-C_5Me_5)Ir^{III} fragment in two differ-

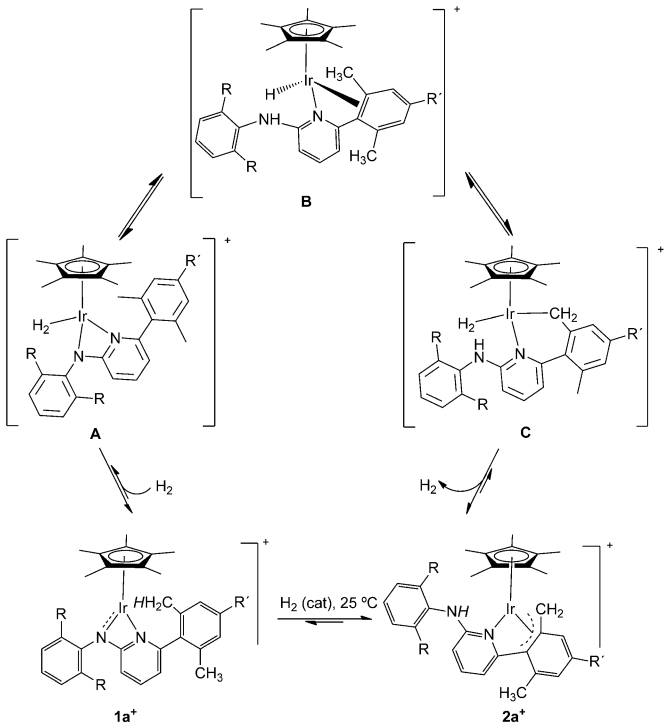

Scheme 9. Proposed mechanism for the H_2-catalysed isomerisation between species $\mathbf{1a}^+$ and $\mathbf{2a}^+$.

ent forms (complexes $\mathbf{1a}^+$–$\mathbf{1d}^+$ and $\mathbf{2a}^+$–$\mathbf{2d}^+$). We have found that H_2 catalyses a prototropic rearrangement, which interchanges a hydrogen atom between one of the 2,6-benzylic positions and the amido site of the aminopyridinate ligands under homogeneous conditions with high efficiency. The process implies reversible formation and cleavage of H–H, C–H and N–H bonds.

Experimental Section

General procedures

Microanalyses were performed by the Microanalytical Service of the Instituto de Investigaciones Químicas (Seville, Spain). Infrared spectra were obtained with a Bruker Vector 22 spectrometer. Mass spectra were obtained at the Mass Spectroscopy Service of the University of Seville. NMR spectra were recorded with a Bruker DRX-500, DRX-400 or DPX-300 spectrometer. Spectra were referenced to external $SiMe_4$ ($\delta = 0$ ppm) by using the residual protic solvent peaks as internal standards (^{1}H NMR experiments) or the characteristic resonances of the solvent nuclei (^{13}C NMR experiments). Spectral assignments were made by routine one- and two-dimensional NMR experiments if appropriate. All manipulations were performed under dry, oxygen-free N_2, by using conventional Schlenk techniques. Crystal structures were determined with a Bruker–Nonius, X8Kappa diffractometer. Metal complex $[IrCl_2Cp^*]_2$[48] and $NaBAr_F$[49] were prepared as previously described. The lithium salts of the Ap ligands were prepared according to published procedures.[14a] The ^{1}H and ^{13}C{^{1}H} NMR spectral data for the BAr_F^- anion in CD_2Cl_2 are identical for all complexes and therefore are not repeated for each individual case below. ^{1}H NMR (500 MHz, CD_2Cl_2): $\delta = 7.75$ (s, 8H; *o*-Ar), 7.58 ppm (s, 4H; *p*-Ar); ^{13}C NMR (125 MHz, CD_2Cl_2): $\delta = 162.1$ (q, ^1J(C,B) = 37 Hz; *ipso*-Ar), 135.3 (*o*-Ar), 129.2 (q, ^2J(C,F) = 31 Hz; *m*-Ar), 124.9 (q, ^1J(C,F) = 273 Hz; CF_3), 117.8 ppm (*p*-Ar). The synthesis and characterisation of ligands **b**–**d**, compounds **1a·Cl**–**1d·Cl**, **[1a]BAr$_F$**–**[1d]BAr$_F$**, **[1a·CO]BAr$_F$**–**[1d·CO]BAr$_F$** and **[1a·L]BAr$_F$** are reported in the Supporting Information.

Synthesis and characterisation

Compound [2a]BAr$_F$: A solution of compound **[1a]BAr$_F$** (0.1 g, 0.065 mmol) in CH_2Cl_2 (5 mL) at 0 °C was treated with H_2 (0.5 bar) and the mixture was stirred for 6 h. ^{1}H NMR analysis of the reaction mixture revealed the formation of complex $\mathbf{2a}^+$ and its isomer $\mathbf{1a}^+$ in approximately a 1:1 ratio. **[2a]BAr$_F$** was separated by fractional crystallisation from Et_2O/hexane mixtures at −23 °C as orange crystals. ^{1}H NMR (500 MHz, CD_2Cl_2, 25 °C): $\delta = 7.72$ (m, ^3J(H,H) ≈ 7.5 Hz, 1H; CH_{Xyl}), 7.59 (t, ^3J(H,H) ≈ 7.5 Hz, 1H; $CH_{Pyridine(Pyr)}$), 7.48 (t, ^3J(H,H) = 8.2 Hz, 1H; $CH_{Diisopropylphenyl(Dipp)}$), 7.45 (t, ^3J(H,H) ≈ 7.5 Hz, 1H; CH_{Xyl}), 7.37 (d, ^3J(H,H) ≈ 7.5 Hz, 1H; CH_{Xyl}), 7.30 (d, ^3J(H,H) = 8.2 Hz, 1H; CH_{Dipp}), 7.01 (d, ^3J(H,H) = 8.2 Hz, 1H; CH_{Dipp}), 6.11 (d, ^3J(H,H) ≈ 7.5 Hz, 1H; CH_{Pyr}), 6.04 (d, ^3J(H,H) ≈ 7.5 Hz, 1H; CH_{Pyr}), 5.94 (s, 1H; NH), 3.68 (d, ^2J(H,H) = 4.5 Hz, 1H; Ir–CHH), 3.19 (septet, ^3J(H,H) ≈ 7.0 Hz, 1H; CH_{iPr}), 2.78 (septet, ^3J(H,H) ≈ 7.0 Hz, 1H; CH_{iPr}), 2.48 (s, 3H; 1×Me_{xyl}), 2.07 (d, ^2J(H,H) = 4.5 Hz, 1H; Ir–CHH), 1.61 (s, 15H; 5×Me_{Cp^*}), 1.30 (d, ^3J(H,H) ≈ 7.0 Hz, 3H; Me_{iPr}), 1.28 (d, ^3J(H,H) ≈ 7.0 Hz, 3H; Me_{iPr}), 1.26 (d, ^3J(H,H) ≈ 7.0 Hz, 3H; Me_{iPr}), 1.01 ppm (d, ^3J(H,H) ≈ 7.0 Hz, 3H; Me_{iPr}); ^{13}C NMR (125 MHz, CD_2Cl_2, 25 °C): $\delta = 157.1$ ($C_{q\text{-}Pyr}$), 154.2 ($C_{q\text{-}Pyr}$), 148.0 ($C_{q\text{-}Dipp}$), 147.7 ($C_{q\text{-}Dipp}$), 146.2 ($C_{q\text{-}Dipp}$), 141.4 (CH_{Pyr}), 137.7 ($C_{q\text{-}Xyl}$), 134.0, 130.0, 129.6, 129.4, 125.3, 125.1 (CH_{Xyl}, CH_{Dipp}), 117.8 (CH_{Pyr}), 107.5 (CH_{Pyr}), 100.4 (Ir–CH_2-C_q), 94.1 (Ir–$C_{q\text{-}xyl}$), 90.2 ($C_{q\text{-}Cp^*}$), 34.9 (d, $^1J(C,H)_{average}$ = 155 Hz; Ir–CH_2), 29.4 (CH_{iPr}), 28.6 (CH_{iPr}), 25.6 (Me_{iPr}), 23.7 (Me_{iPr}), 23.6 (Me_{iPr}), 23.1 (Me_{iPr}), 20.5 (Me_{xyl}), 8.9 ppm (Me_{Cp^*}); IR (Nujol): $\tilde{\nu}$ = 3420 cm^{-1} (br; NH); elemental analysis calcd (%) for $C_{67}H_{56}BF_{24}IrN_2$: C 52.0, H 3.7, N 1.8; found: C 52.0, H 3.7, N 1.8.

Compounds [2b]BAr$_F$–**[2d]BAr$_F$**: See the Supporting Information for synthetic details and characterisation data.

Compound 1a·H:

Method a: Tetramethylpiperidine (5 equiv) was added to an equilibrium mixture of $\mathbf{1a}^+$ and $\mathbf{2a}^+$ in CD_2Cl_2 and the resulting mixture was treated with H_2 (1 atm). The reaction was monitored by ^{1}H NMR spectroscopy until $\mathbf{2a}^+$ had reacted to form **1a·H**.

Method b: To a solution of **1a·Cl** (0.05 g, 0.072 mmol) in THF (5 mL), $NaBH_4$ (≈10 equiv) and methanol (3 mL) were added. The reaction mixture was stirred at RT for 14 h and the colour of the solution changed from orange to yellow. Distilled water (3 mL) was added and the product was extracted with toluene. The organic phase was dried over $MgSO_4$ and the solvent was evaporated under vacuum. Analysis by ^{1}H NMR spectroscopy revealed quantitative conversion into **1a·H**. Note: **1a·H** converts into **1a·Cl** in the presence of chlorinated solvents. An analytically pure sample of **1a·H** could not be obtained due to its slow decomposition in solution when crystallising. ^{1}H NMR (300 MHz, C_6D_6, 25 °C): $\delta = 7.24$ (m, 3H; 3×CH_{Dipp}), 7.05 (m, 1H; CH_{Xyl}), 6.94 (t, ^3J(H,H) ≈ 7.5 Hz, 2H; 2×CH_{Xyl}), 6.73 (t, ^3J(H,H) ≈ 7.5 Hz, 1H; CH_{Pyr}), 5.70 (d, ^3J(H,H) ≈ 7.5 Hz, 1H; CH_{Pyr}), 5.28 (d, ^3J(H,H) ≈ 7.5 Hz, 1H; CH_{Pyr}), 3.97 (septet, ^3J(H,H) = 7.0 Hz, 1H; CH_{iPr}), 3.64 (septet, ^3J(H,H) = 7.0 Hz, 1H; CH_{iPr}), 2.46 (s, 3H; Me_{Xyl}), 2.20 (s, 3H; Me_{Xyl}), 1.41 (s, 15H; 5×Me_{Cp^*}), 1.38 (d, ^3J(H,H) ≈ 7.0 Hz, 6H; 2×Me_{iPr}), 1.27 (d, ^3J(H,H) ≈ 7.0 Hz, 3H; Me_{iPr}), 1.16 (d, ^3J(H,H) ≈ 7.0 Hz, 3H; Me_{iPr}), −7.39 ppm (s, 1H; Ir–H); ^{13}C NMR (75 MHz, C_6D_6, 25 °C): $\delta = 170.7$ ($C_{q\text{-}Pyr}$), 157.2 ($C_{q\text{-}Pyr}$), 146.7 ($C_{q\text{-}Dipp}$), 145.8 ($C_{q\text{-}Dipp}$), 139.9 ($C_{q\text{-}Xyl}$), 138.4 ($C_{q\text{-}Xyl}$), 137.6 ($C_{q\text{-}Dipp}$), 136.5 ($C_{q\text{-}Xyl}$), 134.1 (CH_{Pyr}), 104.8 (CH_{Pyr}), 104.0 (CH_{Pyr}), 128.2 (CH_{Xyl}), 127.9 (CH_{Xyl}), 126.8 (CH_{Xyl}), 124.9 (CH_{Dipp}), 123.8 (CH_{Dipp}), 122.9

(CH_{Dipp}), 84.2 ($C_{q\text{-}Cp^*}$), 27.9 (CH_{iPr}), 26.6 (CH_{iPr}), 25.1 (Me_{iPr}), 24.5 (Me_{iPr}), 24.2 (Me_{iPr}), 23.1 (Me_{iPr}), 20.2 (Me_{Xyl}), 19.7 (Me_{Xyl}), 10.0 ppm (Me_{Cp^*}).

Compound 1b·H: See the Supporting Information for synthetic details and characterisation data.

Compound [2a·CO]BAr_F: CO (g) was bubbled through a solution of **[2a]BAr_F** (0.1 g, 0.065 mmol) in CH_2Cl_2 (5 mL) at RT for 5 min. The solution immediately changed colour from orange to yellow. The solvent was removed under reduced pressure and ^{1}H NMR analysis of the reaction product showed quantitative conversion into **2a·CO$^+$**. The product was washed with pentane and dried under vacuum. ^{1}H NMR (400 MHz, CD_2Cl_2, 25 °C): $\delta = 7.56$ (t, ^3J(H,H) ≈ 7.5 Hz, 1H; CH_{Pyr}), 7.12 (d, ^3J(H,H) ≈ 7.5 Hz, 1H; CH_{Pyr}), 6.22 (d, ^3J(H,H) ≈ 7.5 Hz, 1H; CH_{Pyr}), 7.51 (t, ^3J(H,H) ≈ 7.5 Hz, 1H; CH_{Dipp}), 7.38 (m, ^3J(H,H) ≈ 7.5 Hz, 2H; 2×CH_{Dipp}), 7.30 (t, ^3J(H,H) ≈ 7.5 Hz, 1H; CH_{Xyl}), 7.24 (t, ^3J(H,H) ≈ 7.5 Hz, 1H; CH_{Xyl}), 7.11 (d, ^3J(H,H) ≈ 7.5 Hz, 1H; CH_{Xyl}), 6.68 (s, 1H, NH), 3.78 (d, ^2J(H,H) ≈ 11 Hz, 1H; Ir–CHH), 2.98 (d, ^2J(H,H) ≈ 11 Hz, 1H; Ir–CHH), 3.04 (septet, ^3J(H,H) ≈ 7.0 Hz, 1H; CH_{iPr}), 2.94 (septet, ^3J(H,H) ≈ 7.0 Hz, 1H; CH_{iPr}), 2.34 (s, 3H; Me_{Xyl}), 1.68 (s, 15H; 5×Me_{Cp^*}), 1.27 (d, ^3J(H,H) ≈ 7.0 Hz, 3H; Me_{iPr}), 1.26 (d, ^3J(H,H) ≈ 7.0 Hz, 3H; Me_{iPr}), 1.15 (d, ^3J(H,H) ≈ 7.0 Hz, 3H; Me_{iPr}), 1.14 ppm (d, ^3J(H,H) ≈ 7.0 Hz, 3H; Me_{iPr}); ^{13}C NMR (100 MHz, CD_2Cl_2, 25 °C): $\delta = 168.4$ (Ir–CO), 161.6 ($C_{q\text{-}Pyr}$), 155.0 ($C_{q\text{-}Pyr}$), 147.6 ($C_{q\text{-}Dipp}$), 146.9 ($C_{q\text{-}Dipp}$), 144.8 ($C_{q\text{-}Xyl}$), 140.0 (CH_{Pyr}), 138.4 ($C_{q\text{-}Xyl}$), 137.7 ($C_{q\text{-}Xyl}$), 131.0 ($C_{q\text{-}Dipp}$), 117.7 (CH_{Pyr}), 130.2 (CH_{Dipp}), 129.8 (CH_{Xyl}), 129.0 (CH_{Xyl}), 126.6 (CH_{Dipp}), 126.5 (CH_{Dipp}), 123.2 (CH_{Xyl}), 108.1 (CH_{Pyr}), 101.8 ($C_{q\text{-}Cp^*}$), 29.1 (CH_{iPr}), 28.7 (CH_{iPr}), 24.9 (Me_{iPr}), 24.8 (Me_{iPr}), 23.8 (Me_{iPr}), 23.5 (Me_{iPr}), 21.7 (Me_{Xyl}), 9.7 (dd, ^1J(C,H) = 142 Hz, Ir–CH_2), 8.6 ppm (Me_{Cp^*}); IR (Nujol): $\tilde{\nu} = 3355$ (NH), 2030 cm^{-1} (CO); elemental analysis calcd (%) for $C_{67}H_{56}BF_{24}IrN_2$: C 51.8, H 3.6, N 1.8; found: C 51.6, H 3.8, N 1.6.

Compound [2c·CO]BAr_F: See the Supporting Information for synthetic details and characterisation data.

Computational Details

All calculations were performed by using the Gaussian 09 series of programs[50] with the B3LYP functional.[51,52] An effective core potential[53] and its associated double-ζ LANL2DZ basis set were used for iridium. C, H and N atoms were represented by means of the 6–31G(d,p) basis set (**BS1**).[54–56] Additional calculations were carried out with Truhlar's M06 functional[46] and the SDD core potential for iridium[57] (**BS2**). The latter calculations agree qualitatively with the B3LYP results. The structures of the reactants, intermediates, transition states and products were fully optimised in the gas phase without any symmetry restriction. Frequency calculations were performed on all optimised structures at the same levels of theory to characterise the stationary points and the transitions states, as well as for the calculation of gas-phase zero-point energies (ZPE), enthalpies (*H*), entropies (*S*) and Gibbs energies (*G*) at $T = 298.15$ K. The nature of the intermediates connected by transition states was determined by intrinsic reaction coordinate (IRC) calculations or by perturbing the transition states along the TS coordinate and optimising to a minimum. NBO analysis[58] was performed with the NBO 3.1 program as implemented in Gaussian 09.

X-ray structure analysis

X-ray details are given in the Supporting Information. CCDC-1024982 (ligand **d**), 1024983 (**1a·Cl**), 1024984 (**1b·Cl**), 859075 (**[1a]BAr_F**), 1024985 (**[1d]BAr_F**), 1024986 (**[1a·CO]BAr_F**), 1024987 (**[1a·NH_3]BAr_F**), 1024988 (**[1a·dmap]BAr_F**), 1024989 (**[1a·CNXyl]-BAr_F**), 1024990 (**[1b·CO]BAr_F**), 859076 (**[2a]BAr_F**), 1024991 (**[2b]BAr_F**) and 1024992 (**[2c]BAr_F**) contain the supplementary crystallographic data for this paper. These data can be obtained free of charge from The Cambridge Crystallographic Data Centre via www.ccdc.cam.ac.uk/data_request/cif.

Acknowledgements

Financial support (FEDER contribution and ESF) from the Spanish Ministry of Science (projects CTQ2013-42501-P and Consolider Ingenio 2010 CSD 2007-0006) and the Junta de Andalucía (grant FQM-119 and project P09-FQM-4832) is acknowledged. N.R. and J.L.-S. thank the Spanish Ministry of Science and the University of Seville for two "Ramón y Cajal" contracts.

Keywords: C–H activation · dihydrogen catalysis · iridium · ligand isomerisation · N–H activation

[1] a) Y.-F. Han, G.-X. Jin, *Chem. Soc. Rev.* **2014**, *43*, 2799 – 2823; b) C. Wang, B. Villa-Marcos, J. Xiao, *Chem. Commun.* **2011**, *47*, 9773 – 9785; c) T. Suzuki, *Chem. Rev.* **2011**, *111*, 1825 – 1845; d) M. Albrecht, *Chem. Rev.* **2010**, *110*, 576 – 623; e) S. Kuwata, T. Ikariya, *Dalton Trans.* **2010**, *39*, 2984 – 2992; f) J. Liu, X. Wu, J. A. Iggo, J. Xiao, *Coord. Chem. Rev.* **2008**, *252*, 782 – 809; g) T. Ikariya, A. J. Blacker, *Acc. Chem. Res.* **2007**, *40*, 1300 – 1308.

[2] a) U. Hintermair, S. W. Sheehan, A. R. Parent, D. H. Ess, D. T. Richens, P. H. Vaccaro, G. W. Brudvig, R. H. Crabtree, *J. Am. Chem. Soc.* **2013**, *135*, 10837 – 10851; b) J. Graeupner, U. Hintermair, D. L. Huang, J. M. Thomsen, M. Takase, J. Campos, S. M. Hashmi, M. Elimelech, G. W. Brudvig, R. H. Crabtree, *Organometallics* **2013**, *32*, 5384 – 5390; c) U. Hintermair, S. M. Hashmi, M. Elimelech, R. H. Crabtree, *J. Am. Chem. Soc.* **2012**, *134*, 9785 – 9795; d) R. H. Crabtree, *Organometallics* **2011**, *30*, 17 – 19.

[3] a) C. Zuccaccia, G. Bellachioma, G. Bortolini, A. Bucci, A. Savini, A. Macchioni, *Chem. Eur. J.* **2014**, *20*, 3446 – 3456; b) A. Savini, A. Bucci, G. Bellachioma, L. Rocchigiani, C. Zuccaccia, A. Llobet, A. Macchioni, *Eur. J. Inorg. Chem.* **2014**, 690 – 697; c) C. Zuccaccia, G. Bellachioma, S. Bolaño, L. Rocchigiani, A. Savini, A. Macchioni, *Eur. J. Inorg. Chem.* **2012**, 1462 – 1468; d) D. G. H. Hetterscheid, J. N. H. Reek, *Chem. Commun.* **2011**, *47*, 2712 – 2714; e) W. I. Dzik, S. E. Calvo, J. N. H. Reek, M. Lutz, M. A. Ciriano, C. Tejel, D. G. H. Hetterscheid, B. de Bruin, *Organometallics* **2011**, *30*, 372 – 374.

[4] a) J. F. Hartwig, *Acc. Chem. Res.* **2012**, *45*, 864 – 873; b) N. Kuhl, M. N. Hopkinson, J. Wencel-Delord, F. Glorius, *Angew. Chem. Int. Ed.* **2012**, *51*, 10236 – 10254; *Angew. Chem.* **2012**, *124*, 10382 – 10401; c) G. E. Dobereiner, R. H. Crabtree, *Chem. Rev.* **2010**, *110*, 681 – 703; d) D. Balcells, E. Clot, O. Eisenstein, *Chem. Rev.* **2010**, *110*, 749 – 823; e) D. A. Colby, A. S. Tsai, R. G. Bergman, J. A. Ellman, *Acc. Chem. Res.* **2012**, *45*, 814 – 825; f) G. Song, F. Wang, X. Li, *Chem. Soc. Rev.* **2012**, *41*, 3651 – 3678.

[5] For examples see: a) B. A. Arndtsen, R. G. Bergman, *Science* **1995**, *270*, 1970 – 1973; b) P. Burger, R. G. Bergman, *J. Am. Chem. Soc.* **1993**, *115*, 10462 – 10463; c) J. M. Meredith, R. Robinson, Jr., K. I. Goldberg, W. Kaminsky, D. M. Heinekey, *Organometallics* **2012**, *31*, 1879 – 1887; d) J. Campos, J. López-Serrano, E. Álvarez, E. Carmona, *J. Am. Chem. Soc.* **2012**, *134*, 7165 – 7175.

[6] See, for instance: a) A. J. Blacker, E. Clot, S. B. Duckett, O. Eisenstein, J. Grace, A. Nova, R. N. Perutz, D. J. Taylor, A. C. Whitwood, *Chem. Commun.* **2009**, 6801 – 6803; b) A. Nova, D. J. Taylor, A. J. Blacker, S. B. Duckett, R. N. Perutz, O. Eisenstein, *Organometallics* **2014**, *33*, 3433 – 3442; c) K. Ishiwata, S. Kuwata, T. Ikariya, *J. Am. Chem. Soc.* **2009**, *131*, 5001 – 5009; d) Z. M. Heiden, T. B. Rauchfuss, *J. Am. Chem. Soc.* **2009**, *131*, 3593 – 3600; e) Z. M. Heiden, B. J. Gorecki, T. B. Rauchfuss, *Organometallics* **2008**, *27*, 1542 – 1549; f) Z. M. Heiden, T. B. Rauchfuss, *J. Am. Chem. Soc.* **2007**, *129*, 14303 – 14310; g) J. Campos, U. Hintermair, T. P. Brewster, M. K. Takase, R. H. Crabtree, *ACS Catal.* **2014**, *4*, 973 – 985; h) U. Hintermair, J. Campos, T. P. Brewster, L. M. Pratt, N. D. Schley, R. H. Crabtree, *ACS Catal.* **2014**, *4*, 99 – 108.

[7] a) J. Atzrodt, V. Derdau, T. Fey, J. Zimmermann, *Angew. Chem. Int. Ed.* **2007**, *46*, 7744 – 7765; *Angew. Chem.* **2007**, *119*, 7890 – 7911; b) J. R. Heys, *J. Labelled Compd. Radiopharm.* **2007**, *50*, 770 – 778.

[8] See, for instance: a) J. Campos, M. Rubio, A. C. Esqueda, E. Carmona, *J. Labelled Compd. Radiopharm.* **2012**, *55*, 29 – 38; b) J. Campos, A. C. Esqueda, J. López-Serrano, L. Sánchez, F. P. Cossio, A. de Cozar, E. Álvarez, C. Maya, E. Carmona, *J. Am. Chem. Soc.* **2010**, *132*, 16765 – 16767; c) G. Ciancaleoni, S. Bolaño, J. Bravo, M. Peruzzini, L. Gonsalvi, A. Macchioni, *Dalton Trans.* **2010**, *39*, 3366 – 3368; d) J. A. Brown, S. Irvine, A. R. Kennedy, W. J. Kerr, S. Andersson, G. N. Nilsson, *Chem. Commun.* **2008**, 1115 – 1117; e) R. Corberán, M. Sanaú, E. Peris, *J. Am. Chem. Soc.* **2006**, *128*, 3974 – 3979; f) C. M. Yung, M. B. Skaddan, R. G. Bergman, *J. Am. Chem. Soc.* **2004**, *126*, 13033 – 13043; g) S. R. Klei, J. T. Golden, T. D. Tilley, R. G. Bergman, *J. Am. Chem. Soc.* **2002**, *124*, 2092 – 2093; h) J. T. Golden, R. A. Andersen, R. G. Bergman, *J. Am. Chem. Soc.* **2001**, *123*, 5837 – 5838.

[9] a) G. Zeng, S. Sakaki, K. Fujita, H. Sano, R. Yamaguchi, *ACS Catal.* **2014**, *4*, 1010 – 1020; b) A. Prades, R. Corberán, M. Poyatos, E. Peris, *Chem. Eur. J.* **2009**, *15*, 4610 – 4613; c) A. Prades, R. Corberán, M. Poyatos, E. Peris, *Chem. Eur. J.* **2008**, *14*, 11474 – 11479; d) L. Li, Y. Jiao, W. W. Brennessel, W. D. Jones, *Organometallics* **2010**, *29*, 4593 – 4605; e) A. P. da Costa, M. Viciano, M. Sanaú, S. Merino, J. Tejeda, E. Peris, B. Royo, *Organometallics* **2008**, *27*, 1305 – 1309.

[10] a) Z. Liu, P. J. Sadler, *Acc. Chem. Res.* **2014**, *47*, 1174 – 1185; b) D. P. Smith, H. Chen, S. Ogo, A. I. Elduque, M. Eisenstein, M. Olmstead, R. H. Fish, *Organometallics* **2014**, *33*, 2389 – 2404.

[11] a) J. Campos, M. F. Espada, J. López-Serrano, E. Carmona, *Inorg. Chem.* **2013**, *52*, 6694 – 6704; b) M. Rubio, J. Campos, E. Carmona, *Org. Lett.* **2011**, *13*, 5236 – 5239; c) J. Campos, A. C. Esqueda, E. Carmona, *Chem. Eur. J.* **2010**, *16*, 419 – 422.

[12] J. E. V. Valpuesta, N. Rendón, J. López-Serrano, M. L. Poveda, L. Sánchez, E. Álvarez, E. Carmona, *Angew. Chem. Int. Ed.* **2012**, *51*, 7555 – 7557; *Angew. Chem.* **2012**, *124*, 7673 – 7675.

[13] D. Barr, W. Clegg, R. E. Mulvey, R. Snaith, *J. Chem. Soc. Chem. Commun.* **1984**, 469 – 470.

[14] a) N. M. Scott, T. Schareina, O. Tok, R. Kempe, *Eur. J. Inorg. Chem.* **2004**, 3297 – 3304; b) N. M. Scott, R. Kempe, *Eur. J. Inorg. Chem.* **2005**, 1319 – 1324; c) W. P. Kretschmer, A. Meetsma, B. Hessen, T. Schmalz, S. Qayyum, R. Kempe, *Chem. Eur. J.* **2006**, *12*, 8969 – 8978; d) D. M. Lyubov, C. Döring, S. Y. Ketkov, R. Kempe, A. A. Trifonov, *Chem. Eur. J.* **2011**, *17*, 3824 – 3826.

[15] a) D. M. Lyubov, G. K. Fukin, A. V. Cherkasov, A. S. Shavyrin, A. A. Trifonov, L. Luconi, C. Bianchini, A. Meli, G. Giambastiani, *Organometallics* **2009**, *28*, 1227 – 1323; b) D. M. Lyubov, C. Döring, G. K. Fukin, A. V. Cherkasov, A. S. Shavyrin, R. Kempe, A. A. Trifonov, *Organometallics* **2008**, *27*, 2905 – 2907.

[16] a) E. S. Tamne, A. Noor, S. Qayyum, T. Bauer, R. Kempe, *Inorg. Chem.* **2013**, *52*, 329 – 336; b) A. Noor, T. Bauer, T. K. Todorova, B. Weber, L. Gagliardi, R. Kempe, *Chem. Eur. J.* **2013**, *19*, 9825 – 9832; c) F. R. Wagner, A. Noor, R. Kempe, *Nat. Chem.* **2009**, *1*, 529 – 536; d) A. Noor, G. Glatz, R. Müller, M. Kaupp, S. Demeshko, R. Kempe, *Nat. Chem.* **2009**, *1*, 322 – 325; e) A. Noor, F. R. Wagner, R. Kempe, *Angew. Chem. Int. Ed.* **2008**, *47*, 7246 – 7249; *Angew. Chem.* **2008**, *120*, 7356 – 7359.

[17] a) K. G. Caulton, *New J. Chem.* **1994**, *18*, 25 – 41; b) T. J. Johnson, K. Folting, W. E. Streib, J. D. Martin, J. C. Huffman, S. A. Jackson, O. Eisenstein, K. G. Caulton, *Inorg. Chem.* **1995**, *34*, 488 – 489; c) M. Jiménez-Tenorio, M. C. Puerta, P. Valerga, *Eur. J. Inorg. Chem.* **2004**, 17 – 32; d) C. Tejel, M. P. del Río, M. A. Ciriano, E. J. Reijerse, F. Hartl, S. Záliš, D. G. H. Hetterscheid, N. T. i Spithas, B. de Bruin, *Chem. Eur. J.* **2009**, *15*, 11878 – 11889.

[18] a) R. Noyori, *Angew. Chem. Int. Ed.* **2002**, *41*, 2008 – 2022; *Angew. Chem.* **2002**, *114*, 2108 – 2123; b) C. A. Sandoval, T. Ohkuma, N. Utsumi, K. Tsutsumi, K. Murata, R. Noyori, *Chem. Asian J.* **2006**, *1*, 102 – 110; c) T. Ohkuma, N. Utsumi, K. Tsutsumi, K. Murata, C. Sandoval, R. Noyori, *J. Am. Chem. Soc.* **2006**, *128*, 8724 – 8725.

[19] a) T. Liu, X. Wang, C. Hoffmann, D. L. DuBois, R. M. Bullock, *Angew. Chem. Int. Ed.* **2014**, *53*, 5300 – 5304; b) T. R. Simmons, V. Artero, *Angew. Chem. Int. Ed.* **2013**, *52*, 6143 – 6145; *Angew. Chem.* **2013**, *125*, 6259 – 6261; c) C. S. Letko, Z. M. Heiden, T. B. Rauchfuss, S. R. Wilson, *Inorg. Chem.* **2011**, *50*, 5558 – 5566.

[20] a) M. R. Kelley, J.-U. Rohde, *Dalton Trans.* **2014**, *43*, 527 – 537; b) J. L. McBee, J. Escalada, T. D. Tilley, *J. Am. Chem. Soc.* **2009**, *131*, 12703 – 12713; c) W. H. Bernskoetter, E. Lobkovsky, P. J. Chirik, *Organometallics* **2005**, *24*, 6250 – 6259; d) P. H. M. Budzelaar, N. N. P. Moonen, R. de Gelder, J. M. M. Smits, A. W. Gal, *Eur. J. Inorg. Chem.* **2000**, 753 – 769; e) P. H. M. Budzelaar, R. de Gelder, A. W. Gal, *Organometallics* **1998**, *17*, 4121 – 4123; f) C. Tejel, L. Asensio, M. P. del Río, B. de Bruin, J. A. López, M. A. Ciriano, *Eur. J. Inorg. Chem.* **2012**, 512 – 519; g) C. Tejel, M. P. del Río, L. Asensio, F. J. van den Bruele, M. A. Ciriano, N. T. i Spithas, D. G. H. Hetterscheid, B. de Bruin, *Inorg. Chem.* **2011**, *50*, 7524 – 7534; h) C. Tejel, M. A. Ciriano, M. P. del Río, F. J. van den Bruele, D. G. H. Hetterscheid, N. T. i Spithas, B. de Bruin, *J. Am. Chem. Soc.* **2008**, *130*, 5844 – 5945.

[21] N. Kanematsu, M. Ebihara, T. Kawamura, *Inorg. Chim. Acta* **1999**, *292*, 244 – 248.

[22] a) C. White, A. J. Oliver, P. M. Maitlis, *J. Chem. Soc. Dalton Trans.* **1973**, 1901 – 1907; b) T. M. Gilbert, R. G. Bergman, *J. Am. Chem. Soc.* **1985**, *107*, 3502 – 3507.

[23] a) R. K. Thauer, *Eur. J. Inorg. Chem.* **2011**, 919 – 921, and other articles in this issue on hydrogenases; b) J. C. Gordon, G. J. Kubas, *Organometallics* **2010**, *29*, 4682 – 4701.

[24] a) *Handbook of Heterogeneous Catalysis* (Eds.: G. Ertl, H. Knözinger, F. Schüth, J. Weitkamp), Wiley-VCH, Weinheim, **2008**; b) J. F. Hartwig in *Organotransition Metal Chemistry*, University Science Books, Sausalito, **2010**. A related role for dihydrogen as a co-catalyst in metal-catalysed isomerisation of olefins, or in olefin polymerisation (as a chain-transfer reagent) is also known. See, for example: c) R. Cramer, R. V. Lindsey, *J. Am. Chem. Soc.* **1966**, *88*, 3534 – 3544; d) N. M. G. Franssen, J. N. H. Reek, B. de Bruin, *Chem. Soc. Rev.* **2013**, *42*, 5809 – 5832; e) A. Guyot, R. Spitz, C. Bobichon, J. L. Lacombe in *Catalytic Olefin Polymerization* (Eds.: T. Keii, K. Soga), Elsevier Science, Amsterdam, **1990**, Chap. 3; f) A. S. Hoffman, B. A. Fries, P. C. Condit, *J. Polym. Sci. Part C* **1963**, *4*, 109 – 126.

[25] See, for example: a) U. Eberle, M. Felderhoff, F. Schüth, *Angew. Chem. Int. Ed.* **2009**, *48*, 6608 – 6630; *Angew. Chem.* **2009**, *121*, 6732 – 6757; b) N. Armaroli, V. Balzani, *Angew. Chem. Int. Ed.* **2007**, *46*, 52 – 66; *Angew. Chem.* **2007**, *119*, 52 – 67.

[26] P. Espinet, P. M. Bailey, P. M. Maitlis, *J. Chem. Soc. Dalton Trans.* **1979**, 1542 – 1547.

[27] A. W. Holland, D. S. Glueck, R. G. Bergman, *Organometallics* **2001**, *20*, 2250 – 2261.

[28] See, for example: a) J. Yuan, R. P. Hughes, A. L. Rheingold, *Organometallics* **2009**, *28*, 4646 – 4648; b) A. C. Sykes, P. White, M. Brookhart, *Organometallics* **2006**, *25*, 1664 – 1675; c) J. Zhao, A. S. Goldman, J. F. Hartwig, *Science* **2005**, *307*, 1080 – 1082; d) M. Kanzelberger, X. Zhang, T. J. Emge, A. S. Goldman, J. Zhao, C. Incarvito, J. F. Hartwig, *J. Am. Chem. Soc.* **2003**, *125*, 13644 – 13645.

[29] D. Rais, R. G. Bergman, *Chem. Eur. J.* **2004**, *10*, 3970 – 3978.

[30] a) J. M. Meredith, K. I. Goldberg, W. Kaminsky, D. M. Heinekey, *Organometallics* **2009**, *28*, 3546 – 3551; b) D. Wang, R. J. Angelici, *Inorg. Chem.* **1996**, *35*, 1321 – 1331; c) P. J. Alaimo, B. A. Arndtsen, R. G. Bergman, *J. Am. Chem. Soc.* **1997**, *119*, 5269 – 5270.

[31] A. S. Goldman, K. Krogh-Jespersen, *J. Am. Chem. Soc.* **1996**, *118*, 12159 – 12166.

[32] a) J. C. Thomas, J. C. Peters, *Inorg. Chem.* **2003**, *42*, 5055 – 5073; b) H. V. R. Dias, C. Dash, M. Yousufuddin, M. A. Celik, G. Frenking, *Inorg. Chem.* **2011**, *50*, 4253 – 4255.

[33] a) P. M. Treichel, *Adv. Organomet. Chem.* **1973**, *11*, 21 – 86; b) Y. Yamamoto, *Coord. Chem. Rev.* **1980**, *32*, 193 – 233.

[34] a) S. D. Stults, R. A. Andersen, A. Zalkin, *Organometallics* **1990**, *9*, 115 – 122; b) M. M. Conejo, J. S. Parry, E. Carmona, M. Schultz, J. G. Brennann, S. M. Beshouri, R. A. Andersen, R. D. Rogers, S. Coles, M. Hursthouse, *Chem. Eur. J.* **1999**, *5*, 3000 – 3009.

[35] a) G. J. Kubas, *J. Am. Chem. Soc.* **1984**, *106*, 451 – 452; b) G. J. Kubas, *Metal Dihydrogen and σ-Bond Complexes: Structure, Bonding and Reactivity*, Kluwer Academic/Plenum, New York, **2001**; c) G. J. Kubas, *J. Organomet. Chem.* **2014**, *751*, 33 – 49.

[36] a) R. H. Crabtree, *Angew. Chem. Int. Ed. Engl.* **1993**, *32*, 789 – 805; *Angew. Chem.* **1993**, *105*, 828 – 845; b) P. G. Jessop, R. H. Morris, *Coord. Chem. Rev.* **1992**, *121*, 155 – 284.

[37] a) D. M. Heinekey, A. Lledós, J. M. Lluch, *Chem. Soc. Rev.* **2004**, *33*, 175 – 182; b) S. Sabo-Etienne, B. Chaudret, *Coord. Chem. Rev.* **1998**, *178 – 180*, 381 – 407; c) R. N. Perutz, S. Sabo-Etienne, *Angew. Chem. Int. Ed.* **2007**,

46, 2578 – 2592; *Angew. Chem.* **2007**, *119*, 2630 – 2645; d) M. Besora, A. Lledós, F. Maseras, *Chem. Soc. Rev.* **2009**, *38*, 957 – 966.

[38] a) G. J. Kubas, *Chem. Rev.* **2007**, *107*, 4152 – 4205; b) M. R. Dubois, D. L. Dubois, *Chem. Soc. Rev.* **2009**, *38*, 62 – 72; c) M. R. Dubois, D. L. Dubois, *Acc. Chem. Res.* **2009**, *42*, 1974 – 1982; d) F. Gloaguen, T. B. Rauchfuss, *Chem. Soc. Rev.* **2009**, *38*, 100 – 108.

[39] a) T. M. Gilbert, F. J. Hollander, R. G. Bergman, *J. Am. Chem. Soc.* **1985**, *107*, 3508 – 3516; b) C. S. Letko, Z. M. Heiden, T. B. Rauchfuss, *Eur. J. Inorg. Chem.* **2009**, 4927 – 4930; c) S. M. Whittemore, J. Gallucci, J. P. Stambuli, *Organometallics* **2011**, *30*, 5273 – 5277.

[40] a) R. Asatryan, *Chem. Phys. Lett.* **2010**, *498*, 263 – 269; b) H. Kim, G. A. Ferguson, L. Cheng, S. A. Zygmunt, P. C. Stair, L. A. Curtiss, *J. Phys. Chem. C* **2012**, *116*, 2927 – 2932; c) S. Vogt-Geisse, A. Toro-Labbé, *J. Chem. Phys.* **2009**, *130*, 244308; d) R. K. Joshi, M. Yoshimura, K. Tanaka, K. Ueda, A. Kumar, N. Ramgir, *J. Phys. Chem. C* **2008**, *112*, 13901 – 13904.

[41] E. Sola, A. García-Camprubí, J. L. Andrés, M. Martín, P. Plou, *J. Am. Chem. Soc.* **2010**, *132*, 9111 – 9121.

[42] See Section II of the Supporting Information for full details for these experiments

[43] D. R. Anton, R. H. Crabtree, *Organometallics* **1983**, *2*, 855 – 859.

[44] a) N. M. Weliange, E. Szuromi, P. R. Sharp, *J. Am. Chem. Soc.* **2009**, *131*, 8736 – 8737; b) M. Findlater, W. H. Bernskoetter, M. Brookhart, *J. Am. Chem. Soc.* **2010**, *132*, 4534 – 4535.

[45] See, for example: a) M. Gómez-Gallego, M. A. Sierra, *Chem. Rev.* **2011**, *111*, 4857 – 4963; b) G. Parkin, *J. Labelled Compd. Radiopharm.* **2007**, *50*, 1088 – 1114; c) K. E. Janak in *Comprehensive Organometallic Chemistry, 3rd ed.* (Eds.: D. M. P. Mingos, R. H. Crabtree), Elsevier, Amsterdam, **2007**, Chap. 1.20; d) See chapter 7 of Ref. [35b]].

[46] Y. Zhao, D. G. Truhlar, *Theor. Chem. Acc.* **2008**, *120*, 215 – 241.

[47] No transition state was located that connects the two conformers at this level of theory, however previous calculations based on the simplified model **Cp·1b**$^+$ predict a low energy barrier of 12.0 kcal mol^{-1} for this transformation.

[48] C. White, A. Yates, P. M. Maitlis, D. M. Heinekey, *Inorg. Synth.* **1992**, *29*, 228 – 234.

[49] M. Brookhart, B. Grant, A. F. Volpe, *Organometallics* **1992**, *11*, 3920 – 3922.

[50] Gaussian 09 (Revision B.01), M. J. Frisch, G. W. Trucks, H. B. Schlegel, G. E. Scuseria, M. A. Robb, J. R. Cheeseman, G. Scalmani, V. Barone, B. Mennucci, G. A. Petersson, H. Nakatsuji, M. Caricato, X. Li, H. P. Hratchian, A. F. Izmaylov, J. Bloino, G. Zheng, J. L. Sonnenberg, M. Hada, M. Ehara, K. Toyota, R. Fukuda, J. Hasegawa, M. Ishida, T. Nakajima, Y. Honda, O. Kitao, H. Nakai, T. Vreven, J. A. Montgomery, Jr., J. E. Peralta, F. Ogliaro, M. Bearpark, J. J. Heyd, E. Brothers, K. N. Kudin, V. N. Staroverov, R. Kobayashi, J. Normand, K. Raghavachari, A. Rendell, J. C. Burant, S. S. Iyengar, J. Tomasi, M. Cossi, N. Rega, J. M. Millam, M. Klene, J. E. Knox, J. B. Cross, V. Bakken, C. Adamo, J. Jaramillo, R. Gomperts, R. E. Stratmann, O. Yazyev, A. J. Austin, R. Cammi, C. Pomelli, J. W. Ochterski, R. L. Martin, K. Morokuma, V. G. Zakrzewski, G. A. Voth, P. Salvador, J. J. Dannenberg, S. Dapprich, A. D. Daniels, Ö. Farkas, J. B. Foresman, J. V. Ortiz, J. Cioslowski, D. J. Fox, Gaussian, Inc., Wallingford CT, **2010**.

[51] A. D. Becke, *J. Chem. Phys.* **1993**, *98*, 5648 – 5652.

[52] C. Lee, W. Yang, R. G. Parr, *Phys. Rev. B* **1988**, *37*, 785 – 789.

[53] P. J. Hay, W. R. Wadt, *J. Chem. Phys.* **1985**, *82*, 299 – 310.

[54] W. J. Hehre, R. Ditchfield, J. A. Pople, *J. Phys. Chem.* **1972**, *56*, 2257 – 2261.

[55] P. C. Hariharan, J. A. Pople, *Theor. Chim. Acta.* **1973**, *28*, 213 – 222.

[56] M. M. Francl, W. J. Pietro, W. J. Hehre, J. S. Binkley, M. S. Gordon, D. J. DeFrees, J. A. Pople, *J. Chem. Phys.* **1982**, *77*, 3654 – 3665.

[57] D. Andrae, U. Haeussermann, M. Dolg, H. Stoll, H. Preuss, *Theor. Chem. Acc.* **1990**, *77*, 123 – 141.

[58] A. E. Reed, L. A. Curtis, F. Weinhold, *Chem. Rev.* **1988**, *88*, 899 – 926.

Received: September 19, 2014
Published online on ■■ ■■, 0000

FULL PAPER

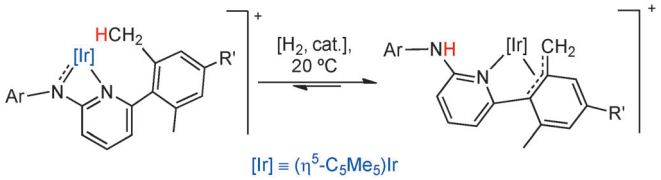

[Ir] ≡ (η^5-C_5Me_5)Ir

Aminopyridinate (Ap) complexes of composition [Ir(Ap)(η^5-C_5Me_5)]$^+$ exist in the form of two isomers **1a**$^+$–**1d**$^+$ and **2a**$^+$–**2d**$^+$ that equilibrate in the presence of H_2 by means of a reversible prototropic rearrangement within the Ap ligand. The isomerisation reaction is catalysed by dihydrogen and implies reversible formation and cleavage of H–H, C–H and N–H bonds.

Isomerisation

*A. Zamorano, N. Rendón, J. López-Serrano, J. E. V. Valpuesta, E. Álvarez, E. Carmona**

■■ – ■■

Dihydrogen Catalysis of the Reversible Formation and Cleavage of C–H and N–H Bonds of Aminopyridinate Ligands Bound to (η^5-C_5Me_5)Ir^{III}